Failure Mechanism of Reinforced Concrete Structural Walls with and without Confinement

D. Escolano-Margarit
University of Granada, Granada, Spain

A. Klenke & S. Pujol
Purdue University, West Lafayette, Indiana, US

A. Benavent-Climent
University of Granada, Granada, Spain

SUMMARY
This paper presents the results of cyclic loading tests on two large-scale reinforced concrete structural walls conducted at Purdue University. One of the walls had confinement reinforcement meeting ACI-318-11 requirements while the other wall did not have any confinement reinforcement. The walls were tested as part of a larger study aimed at developing formulations to estimate the drift capacity of structural walls. This paper discusses the effects of confinement on the displacement capacity of two test walls. Distributions of unit strain and curvature obtained with a dense array of non-contact coordinate-tracking targets are also presented.

Keywords: Structural Wall, Cyclic Test, Plastic Hinge.

1. INTRODUCTION

Structural walls have been commonly used during the past decades as a lateral-load resisting system. But field observations made after the Maule, Chile, Earthquake of 2010 have shown that structural walls can be vulnerable to rather modest displacement demands. The question to be addressed is what factors affect the displacement capacity of a wall? It is clear that a flexural mode of failure is preferable to brittle shear failure. But even walls controlled by flexure can have limited drift capacity. In the case of these walls, it is common to assume that inelastic curvatures concentrate at the wall base in what is referred to as "plastic hinges." For the sake of simplicity, the inelastic curvatures, ϕ_i, in a plastic hinge are 1) computed assuming that strains are linearly distributed across the wall section and 2) assumed to be constant over the length of the plastic hinge, l_p. But this simplicity comes at a price: how is one to estimate (or even measure) a quantity as abstract as the length of the idealized hinge? And even if one did so, what is the limiting curvature? The traditional strain limits of 0.003 and 0.004 are certainly stringent, but being stringent is not always required or necessary. In the case of the length of the idealized hinge, researchers have proposed a plethora of expressions during the last decades for RC columns and beams starting with work at PCA and University of Illinois and continuing more recently by Bae & Bayrak (2008), Priestly & Park (1987) and Sheikh & Khoury (1993). But we have found less information about the case of structural walls. Moehle & Wallace (1992) suggested that the length of the idealized hinge can be assumed to be half the wall length. Dazio et al (2009) suggested several strain limits based on the curvature measured at the base of six shear walls during a cyclic loading test. Bohl & Adebar (2011) proposed plastic hinge lengths based on the results of non-linear finite element analyses. This paper presents the results from two large-scale reinforced concrete structural wall tests conducted at Purdue University. One of the specimens had confinement reinforcement in the boundary elements but the other one did not. The test results show that the concepts of plastic hinge and curvature, while convenient for design, are of limited use if one needs to relate displacement and mean unit strains.

2. EXPERIMENTAL INVESTIGATION

Two large-scale reinforced concrete structural walls were tested under monotonic cyclic loads at Purdue University. One of the specimens (W-MC-C) had confinement reinforcement while the other (W-MC-N) did not have any confinement reinforcement.

2.1. Structural wall design

Specimen W-MC-C (Fig. 1) was designed to meet ACI-318-11 (ACI Committee 318 (2011)) confinement reinforcement requirements. The longitudinal reinforcement was 4 #8 bars in each boundary element and 6 #4 bars in the web. The confinement reinforcement was #2 hoops spaced at 2.5 in center to center in the lower 5 ft of the wall. Ties were cut from #3 bars and were spaced at 5 in. They had 135 degree hooks. Specimen W-MC-N (Fig. 1) had the same layout except that is had no confinement reinforcement. Both specimens had mechanical couplers at the base of the wall to splice all longitudinal bars from the wall and bars anchored in the footing. Measure values of the yield stress, f_y, and ultimate stress, f_u, of the reinforcement, as well as the compressive strength, f'_c, tensile strenth from splitting cylinder tests, f_{ct}, and Module of elasticity, E_c, of the concrete are listed in Table1.

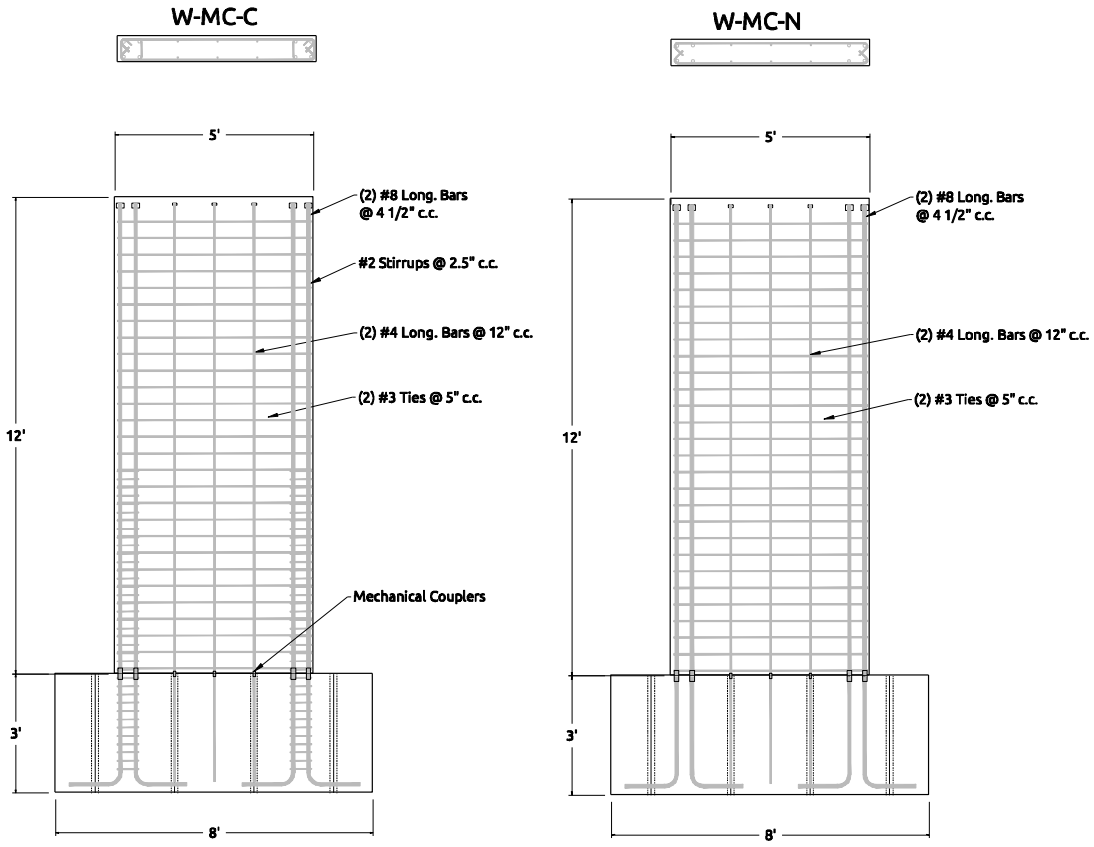

Figure 1. Geometry and reinforcement

Table 1: Mechanical properties of materials

Steel			Concrete							
				WMCC			WMCN			
Bar Size #	f_y (ksi)	f_{su} (ksi)		f'_c (psi)	f_{ct} (psi)	E_c (ksi)	f'_c (psi)	f_{ct} (psi)	E_c (ksi)
2	69	80	Footing 1	5105	453	3645	5059	392	3645
3	70	98	Footing 2	4606	473	3224	4570	395	3604
4	62	90	Lift 1 (0-6.5ft)	4455	468	3637	4467	406	3569
8	67	94	Lift 2 (6.5 -11ft)	5033	427	3873	5130	423	3740
9	63	98	Lift 3(11-12 ft)	4790	421	4010	5068	445	3990

3. SET-UP, INSTRUMENTATION AND LOADING HISTORY

The structural walls were fixed to the strong floor using 8 1-¼-in diameter post-tensioning bars With a total clamping force of 960 kips. The walls were loaded using two hydraulic actuators with hinges at both ends. The resultant from the actuator forces acted at approximately 130.5 in. from the top of the foundation block. The axial load was applied using four post-tensioning bars connected to foundation. The bars were post-tensioned by 4 jacks placed at the top of the walls. The pressure in the jacks was controlled to keep the axial load nearly constant through the tests. Two load cells (LC1 and LC2 in Fig. 3) were used to monitor the axial load. Steel tubes were placed on either side of the wall, 10 ft from the top of the foundation block and parallel to the loading direction, to prevent the out of plane movement of the walls exceeding approximately 1/8 in. Fig. 2 shows the experimental set up.

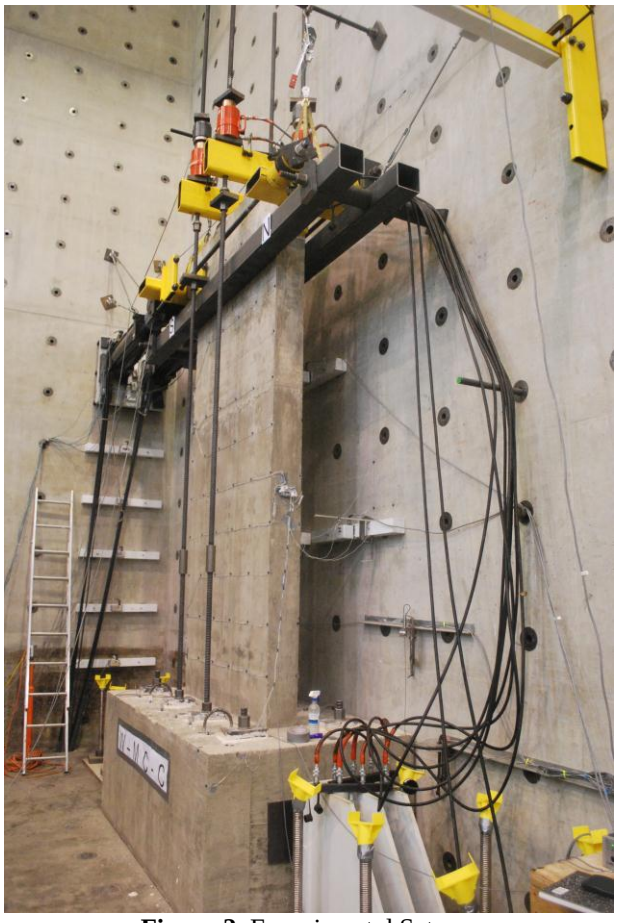

Figure 2. Experimental Set-up.

3.1. Instrumentation

During each cycle loads and displacements, was measured with the following sensors (Fig. 3): (i) Load cells LC1 and LC2 measured the applied load. (ii) Load cells LC3 and LC4 measured the axial load. (iii) Optical encoders, ENC 1 to 8 and 12, measured the displacements in the direction of the loading. (iv)The coordinates of 62 non contact coordinate-tracking targets forming a 1 by 1 ft grid (Fig. 3) were also measured at of the peak of each cycle using an Optotrack Pro system. The labels and positions of instruments are shown in Fig. 3.

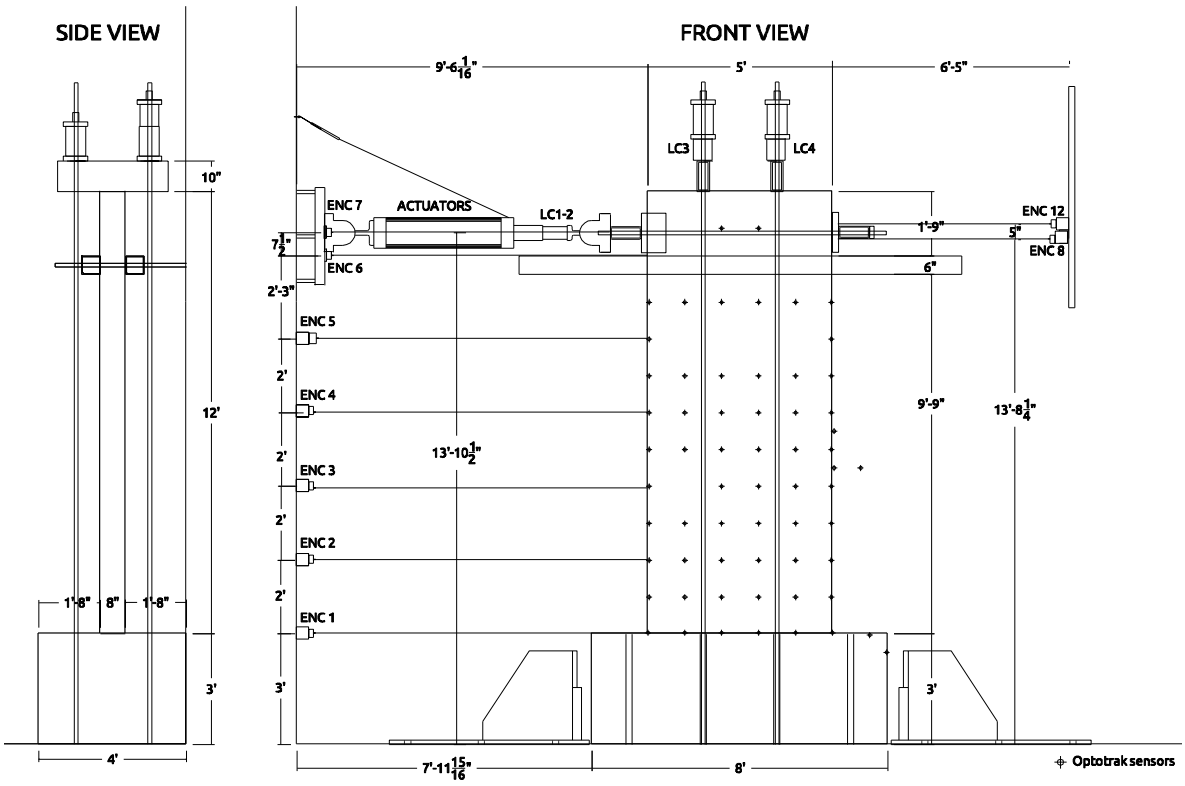

Figure 3. Instrumentation

3.2. Loading history

The axial load was 200 kip and was kept approximately constant during the tests. The imposed horizontal displacement history at the top of the walls is shown in Fig. 4. Three cycles were applied at each drift level. The drift ratio targets were 0.12, 0.25, 0.5, 0.75, 1.0, 1.50, 2, 2.5 and 3.0% (expressed as percentage of the wall height). Because of a failure in the control system, only one cycle at 0.75% and no cycles at 1% were applied to wall W-MC-N.

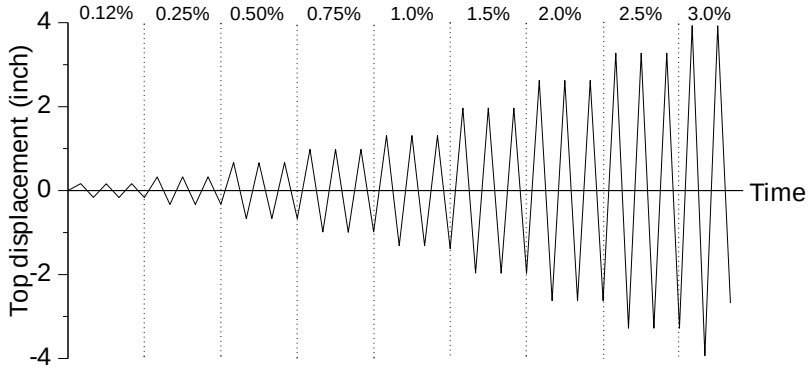

Figure 4. Loading history

4. TESTS RESULTS.

4.1. Specimen W-MC-C

First cracking was observed in cycle #1 at a load of 46 kips and a displacement of 0.17 in. First yield occurred in cycle #10 at a load of 137 kips and a displacement of nearly 1 in. Splitting cracks and spalling at the base of the boundary elements was first observed in cycle #11. The peak lateral load (163 kips) was reached in cycle #25 at 3.9 in. of displacement. The wall failed in cycle #26 when the boundary element failed in compression. During the failure all the boundary reinforcement buckled in the same direction (out of plane). Fig. 7a shows the load-top displacement hysteresis curve measured. Fig. 5 shows photographs of the crack patterns at the base for key response states. The maximum crack widths measured during the tests were 0.005, 0.03 and 0.15 in. at first cracking (0.12%), first yield (0.75%) , and limiting displacement. (3%)

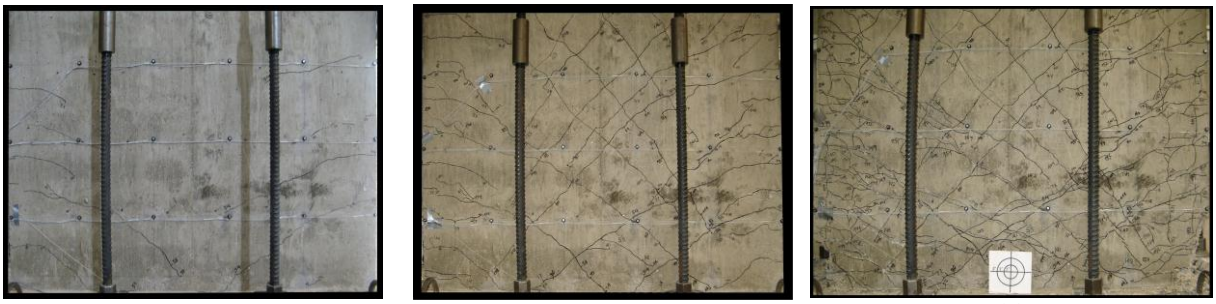

(a) (b) (c)

Figure 5. Crack patterns for limit states: (a) Flexural cracking (0.12%) (b) First yield (0.75%) (c) Limiting displacement (3%)

4.2. Specimen W-MC-N

First cracking was observed in cycle #1 at a load of 42 kips and a displacement of 0.16 in. First yield occurred in cycle #10 at a load of 137 kips and a displacement of nearly 1 in. Splitting cracks and spalling at the base of the boundary elements was first observed in cycle #9. The peak lateral load (155 kips) was reached in cycle #14 at 2.6 in. of displacement. The wall failed in cycle #19 as the bars in one of the boundary elements buckled (away from the center of the wall). During the failure all the boundary reinforcement buckled in the same direction (out of plane). Fig. 7b shows the load-top displacement hysteresis curve measured. Fig. 6 shows photographs of the crack patterns at the base for key response states. The maximum crack widths measured during the tests were 0.005, 0.025 and 0.15 in. at first cracking (0.12%), first yield (0.75%), and limiting displacement (2.5%).

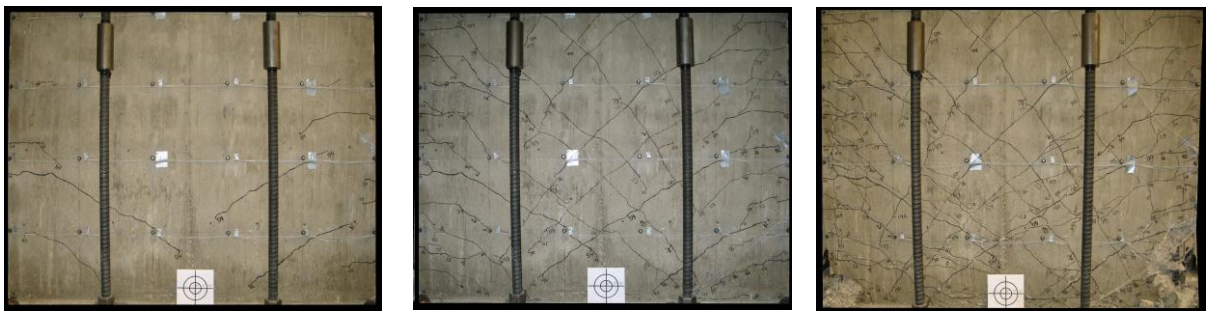

(a) (b) (c)

Figure 6. Crack patterns for limit states: (a) Flexural cracking (0.12%) (b) First yield (0.75%) (c) Limiting displacement (2.5%).

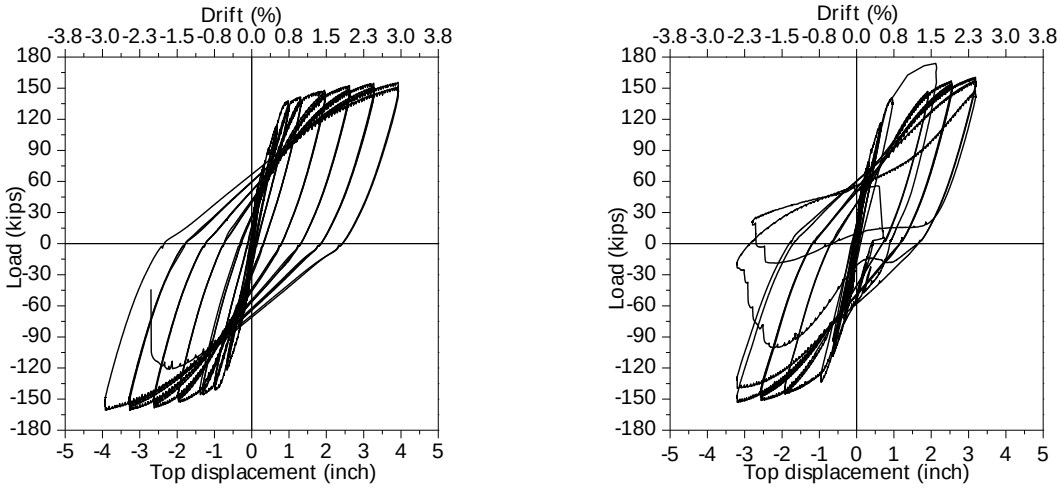

(a) (b)

Figure 7. Load versus top displacement hysteresis curve (a) W-MC-C (b) W-MC-N

5. DISCUSSION OF TEST RESULTS.

5.1. Limit states.

Table 2 summarizes the values of displacement and force for i) flexural cracking (Δ_{cr} and V_{cr}) ii) First yield Δ_y and V_y, and iii) (first peak at) limiting displacement Δ_u and V_u. The limiting displacement was selected as the maximum displacement reached before failure. The numbers in Table 2 and the envelopes in Fig. 8 show that:

1) As expected, the response of the two walls was nearly identical up to yield
2) The limiting displacement for the wall with confinement (W-MC-C) was larger that that of the wall without confinement (W-MC-N). But it is interesting that the difference between these two displacements did not exceed 0.5% of the height of the walls.

Table 2: Δ-V, Member limit states.

W-MC-C						W-MC-N					
Δ_{cr} (inch)	V_{cr} (inch)	Δ_y (inch)	V_y (kips)	Δ_u (inch)	V_u (kips)	Δ_{cr} (inch)	V_{cr} (kips)	Δ_y (inch)	V_y (kips)	Δ_u (inch)	V_u (kips)
0.16	58	0.98	141	3.93	161	0.16	56.3	0.96	138	3.18	157

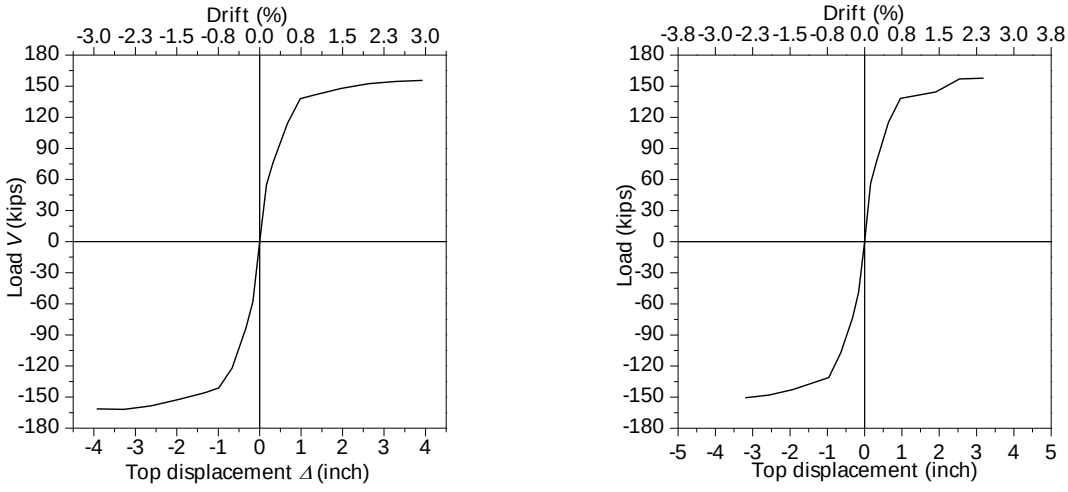

(a) (b)

Figure 8. Load versus top displacement envelope curves. (a) W-MC-C (b) W-MC-N

5.3. Normal Strain distribution.

To speak of strain (or rather unit strain) in reinforced concrete and after cracking requires imagination. Strictly, we should speak of average deformation per unit length. But we keep with the norm and call these unit deformation strains here to keep things brief. Fig. 9 shows contours of the strains measured using the infrared targets in the lower 60 in. of wall shown in Fig. 3. Overall, the distribution of strain appears to have been remarkably similar in both walls. Of course there are differences. But more interestingly, in both walls the strains in the boundary in compression seem to have concentrated within approximately 18 in. from the base (approximately twice the wall thickness (Takahashi (2011)) and 1.5 times the neutral axis depth) both at a drift ratio of 0.75% and at a drift ratio of 2%. In the boundary in tension the strains spreaded over a region at least twice as tall (with a height nearly equal to half the wall length).

Fig. 10 show the distributions of normal unit strains due to flexural deformations measured on the edges of the walls at other drift ratios. These figures show clearly that the "spread of plasticity" –as it is often called- it is very different on the side of the wall in tension and the side of the wall in compression. The concepts of curvature and plastic hinge do not help explain these observations.

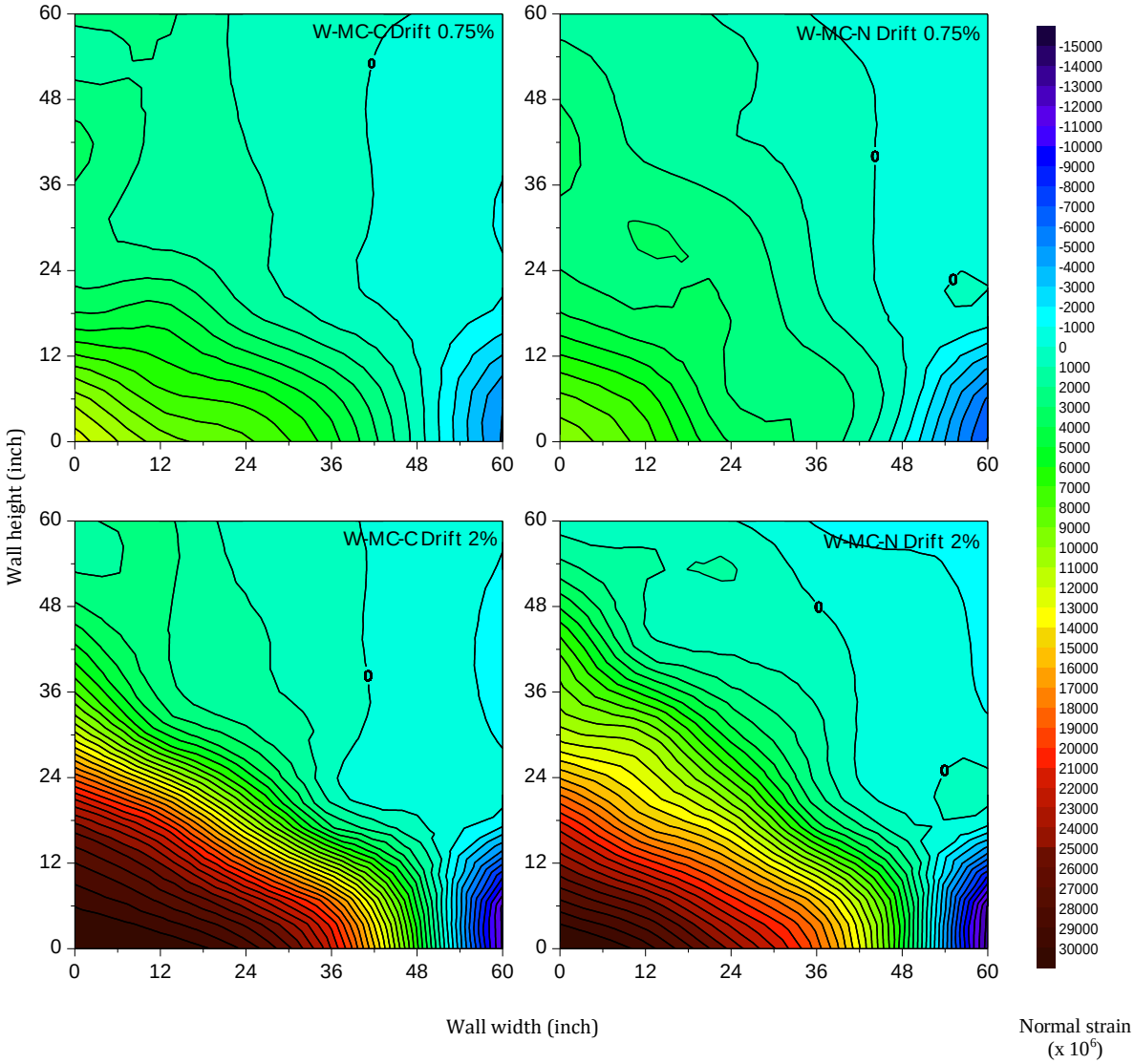

Figure 9. Strain distribution near wall base.

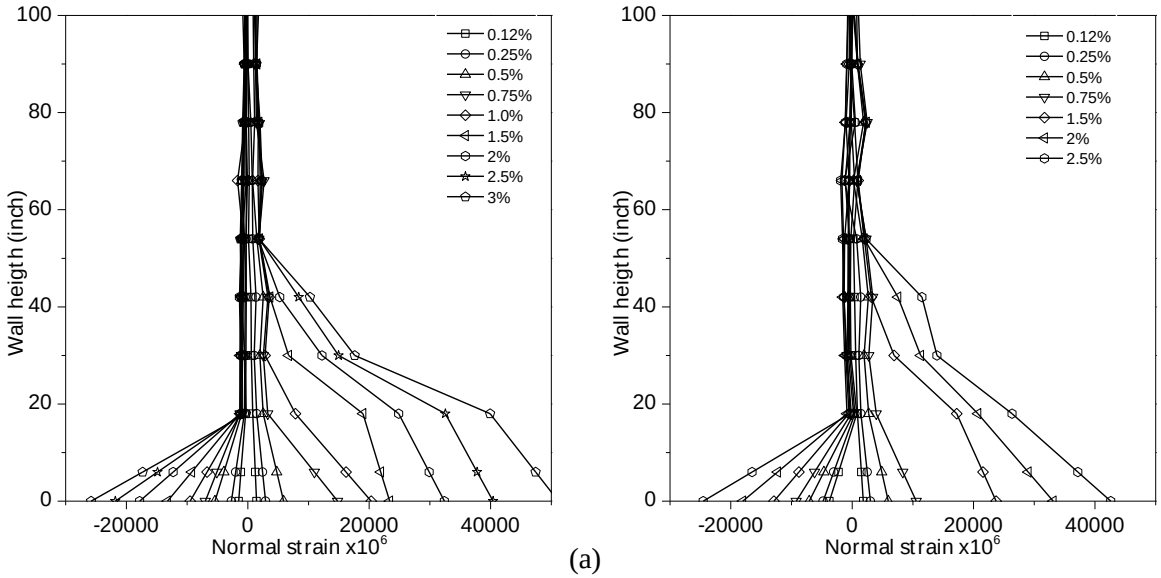

Figure 10. Normal strain distribution over the height at different drift ratios. (a) W-MC-C (b) W-MC-N

5.2. Curvature Distribution.

Unit curvature was computed as the ratio of change in angle to height difference using the outer targets in the non-contact sensor grid shown in Fig. 3. Fig. 11 shows the distribution of unit curvature along the wall height computed as the mean values of the unit curvatures obtained for the 3 cycles at each drift level. The unit curvatures at the base were linearly extrapolated from the values obtained at 6 and 18 inch. The maximum curvature observed at a given drift was almost equal for both specimens. Near the base of the wall, the curvature profile approaches a triangle of height equal to $0.5h_w$ (30 in.).

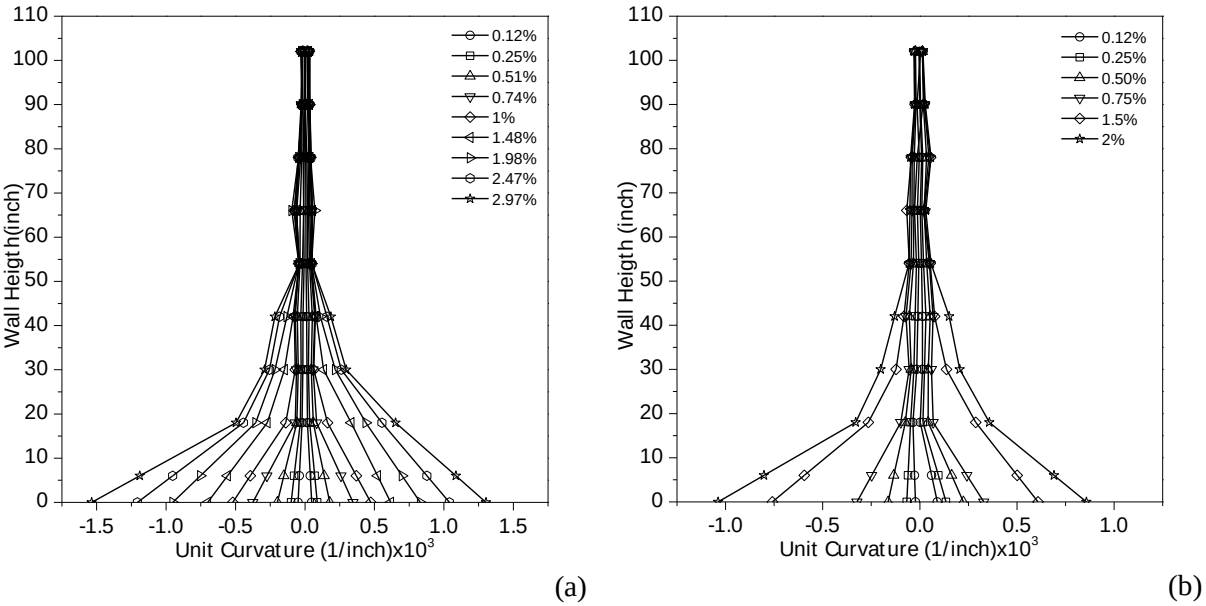

Figure 11. Unit Curvature distribution over the height at different drift ratios. (a) W-MC-C (b) W-MC-N

6. CONCLUSIONS.

Two large-scale reinforced concrete structural walls were tested. The walls had height-to-length ratios of approximately 2.2. One of the walls had confinement reinforcement meeting ACI-318-11 requirements while the other wall did not have any confinement reinforcement. As expected, the confinement reinforcement increased the lateral displacement capacity of the wall. The increase in limiting drift was 0.5% of the wall height (the wall with confinement failing at a displacement equal to 3% of its height).

Measurements made with a dense array of non-contact sensors indicated that inelastic unit curvatures had a nearly linear distribution near the wall base. The height of the region in which these curvatures concentrated was nearly half the wall length. The concepts of curvature and plastic hinge, nevertheless, do not help explain measurements indicating that the lengths of the regions in which inelastic compressive and tensile strains concentrate (on opposite sides of the wall) are radically different from one another. Tensile strains concentrated in a length approximately equal to half the wall height (30 in.) while compressive strains concentrated in a length approximately equal to twice the wall thickness and 1.5 times the neutral axis depth (approximately 18 in).

ACKNOWLEDGEMENT

Financial support from ERICO Inc., the Concrete Reinforcing Steel Institute, the Spanish Government, Projects Ref. BIA 2008/00050 and BIA2011-26816 and from the European Union (*Fonds Europeen de Development Regional*).) is acknowledged.

REFERENCES

ACI Committee 318 (2011). 318-11: Building Code Requirements for Structural Concrete and Commentary. American Concrete Institute.

Bae, S. & Bayrak, O. (2008). Plastic hinge length of reinforced concrete columns. *ACI Structural Journal*, ***105*:3**, 290-30.

Bohl, A., & Perry, A. (2011). Plastic hinge lengths in high-rise concrete shear walls. *ACI Structural Journal*, **108:2**, 148-157.

Dazio, A., Beyer, K., & Bachmann, H. (2009). Quasi-static cyclic tests and plastic hinge analysis of RC structural walls. *Engineering Structures*. **31:7**, 1556-1571. doi:10.1016/j.engstruct.2009.02.018

Priestly, M. J. N. & Park, R. (1987). Strength and Ductility of Concrete Bridge Columns Under Seismic Loading. *Aci Structural Journal*, **January-February**, 61-76.

Sheikh, S. A., & Khoury, S. S. (1993). Confined concrete columns with stubs. *ACI Structural Jour*nal, **90**, 414–414.

Takahashi, S. (2011). Flexural drift capacity of reinforced concrete walls which fails in flexural compression failure. The 13th Taiwan-Japan-Korea Joint Seminar on Earthquake Engineering for Building Structures

Wallace, J. W. & Moehle, J. P. (1992) Ductility and Detailing Requirements of Bearing Wall Buildings. *Journal of Structural Engineering ASCE*, **118: 6**, 1625-1644.